Macromolecules

ARTICLE

pubs.acs.org/Macromolecules

A Low-Bandgap Conjugated Polymer Based on Squaraine with Strong Two-Photon Absorption

Qinqin Shi,[†,§] Wei-Qiang Chen,[‡] Junfeng Xiang,[†] Xuan-Ming Duan,[*,‡] and Xiaowei Zhan[*,†]

[†]Beijing National Laboratory for Molecular Sciences and Key Laboratory of Organic Solids, Institute of Chemistry, Chinese Academy of Sciences, Beijing 100190, China

[‡]Laboratory of Organic Nanophotonics and Key Laboratory of Photochemical Convention and Functional Materials, Technical Institute of Physics and Chemistry, Chinese Academy of Sciences, Beijing 100190, China

[§]Graduate University of Chinese Academy of Sciences, Beijing 100049, China

S *Supporting Information*

ABSTRACT: A new low-bandgap π-conjugated D−A copolymer of squaraine and pyridopyrazine (**P1**) and a new small molecule squaraine−pyridopyrazine model compound (**P2**) were synthesized and compared. **P1** and **P2** exhibit strong NIR absorption and low bandgap (1−1.3 eV). **P2** in solution shows an intense and sharp absorption peak at 764 nm, while **P1** in solution exhibits a red-shifted and broad absorption peak at 808 nm. The HOMO and LUMO levels of **P1** were estimated to be −5.02 and −4.15 eV, while the HOMO and LUMO levels of **P2** were estimated to be −5.27 and −3.22 eV, respectively. Polymer **P1** exhibits strong two-photon absorption (2PA) at telecommunication wavelengths with 2PA cross sections per repeat unit as high as 2300 GM, 3−5 times that for the small molecule **P2**. The higher HOMO, the lower LUMO levels, lower bandgap, red-shifted absorption, and stronger two-photon absorption of **P1** are attributed to higher degree of conjugation and delocalization of π-electrons in the polymer.

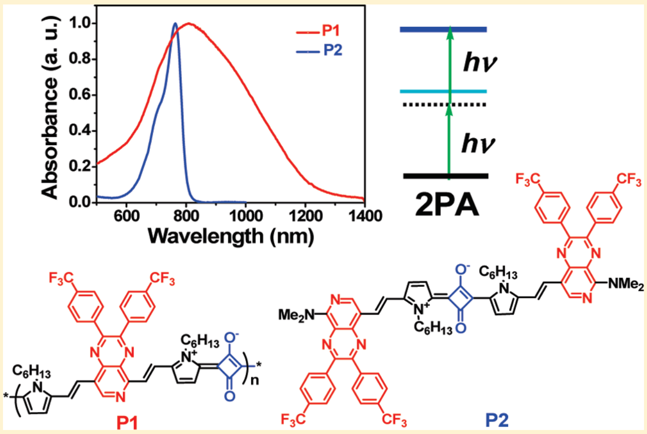

INTRODUCTION

Squaraine dyes are generally synthesized by condensation of electron-rich aromatic or heterocyclic compounds such as pyrrole with squaric acid.[1,2] Squaraines typically have a donor (D)−acceptor (A)−donor (D), resonance-stabilized zwitterionic structure.[3,4] Their main characteristic is the sharp and strong low-energy absorption ($\varepsilon > 10^5$ L mol^{-1} cm^{-1}) frequently associated with a strong fluorescence in the visible to near-IR (NIR) region in solution.[5] Squaraines are usually photostable due to the resonance zwitterionic structure.[4] Since squaraine dyes were first reported in 1965 by Triebs and Jacob,[6] squaraines are widely used in the design of a variety of electronic and photonic materials for applications such as photoconductivity,[7] data storage,[8] light-emitting field-effect transistors,[9] nonlinear optics,[10] solar cells,[11,12] fluorescence probes,[13−17] and photodynamic therapy.[18]

Two-photon absorption (2PA) materials have attracted considerable attention due to their potential applications in three-dimensional (3D) data storage, 3D microfabrication, optical limiting, optical pulse suppression, frequency up-converted lasing, bioimaging, and photodynamic therapy.[19−23] Although squaraine dyes have a small detuning energy, the sharp and strong one-photon absorption (1PA) band endows them with large 2PA cross sections (δ). Schwoerer et al. reported that D−A−D squaraine oligomers exhibited δ of 5000 GM (1 GM = 1 × 10^{-50} cm^4 s^{-1}) at 820−890 nm.[24] Later, Marder et al. reported extended squaraine dyes with δ values as high as 33 000 GM, which is the highest reported for squaraine-based dyes.[25] Because of substantial electronic coupling between the porphyrin and squaraine moieties, a triad of porphyrin−squaraine−porphyrin also displayed a very high δ over a wide range of wavelengths.[26,27] Since low-bandgap squaraine dyes are not suitable for the 2PA application in optical limiting and photoinitiator, some indolic squaraines with large optical bandgap were proposed, and δ of 450 GM was obtained.[28,29]

Polysquaraines were theoretically and experimentally considered as suitable candidates for low-bandgap semiconducting polymers.[30−32] Havinga et al. reported the first soluble squaraine-based polymer.[33] Ajayaghosh et al. found that polysquaraines exhibited intrinsic conductivity of 5.3 × 10^{-4} S cm^{-1},[34−37] and they have also reported polysquaraines used for the detection

Received: February 19, 2011
Revised: April 8, 2011
Published: April 15, 2011

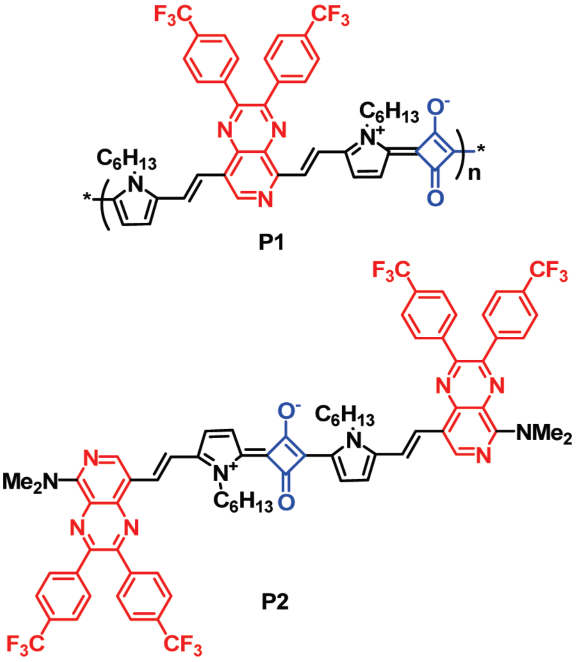

Figure 1. Chemical structures of **P1** and **P2**.

of cations.[38,39] However, to our knowledge, there have been no reports on polysquaraines for use in 2PA.

In recent years, fused-ring pyrazines have been proven to be promising candidates for n-type semiconductors due to the existence of electron-withdrawing imine nitrogen atoms, some of which exhibit high electron mobilities.[40−42] We reported that a copolymer of porphyrin and 2,3-bis(4-trifluoromethylphenyl)-pyrido[3,4-*b*]pyrazine exhibited strong two-photon absorption with δ value of 3200 GM at telecommunication wavelengths.[43] Here we report synthesis of a new low-bandgap π-conjugated D−A copolymer of squaraine and pyridopyrazine (**P1**, Figure 1). **P1** exhibits strong NIR absorption and large 2PA cross sections at telecommunication wavelengths. We also compared this D−A copolymer with a small molecule squaraine−pyridopyrazine model compound (**P2**, Figure 1) and found 3−4 times 2PA enhancement in **P1** relative to its small molecule counterpart **P2**.

RESULTS AND DISCUSSION

Synthesis and Characterization of P1 and P2. Synthetic routes to the squaraine dyes **P1** and **P2** are shown in Scheme 1. The 2-vinylpyrrole intermediate (**1**) was synthesized by Horner−Hammond condensation of 1-hexylpyrrole-2-carbaldehyde with PPh_3MeBr. The vinylpyrrole-disubstituted intermediate **2** was synthesized by Heck coupling reaction between compound **1** and 5,8-dibromo-2,3-bis(4-trifluoromethylphenyl)pyrido[3,4-*b*]pyrazine (**0**). To our surprise, vinylpyrrole-monosubstituted compound **3** was isolated in 38% yield as a byproduct. This unexpected product was confirmed by HR-MS, ^{1}H NMR, and selective 1D NOE NMR (Figures S1−S3, Supporting Information). A similar phenomenon was reported in the literature.[44] We have not yet fully explored this observation. We speculate that trace $HNMe_2$ (from hydrolysis of DMF) in the solvent DMF reacts with compound **0** in the presence of the base to afford 5-dimethylamino-8-bromo-2,3-bis(4-trifluoromethylphenyl)pyrido-[3,4-*b*]pyrazine (**4**, Scheme S1, Supporting Information). Heck coupling reaction between compounds **1** and **4** gave **3**. At compound **1**/compound **0** = 1:1 (mole ratio), tiny **2** (ca. 5%) and **4** (main product) were obtained. At compound **1**/compound **0** = 3:1 (mole ratio), **2** and **3** were obtained. At compound **1**/compound **0** = 4:1 (mole ratio), **2** was the main product (60% yield) (Scheme S1, Supporting Information). The final products **P1** and **P2** were synthesized by condensation of pyridopyrazine-substituted pyrrole species with squaric acid in refluxing *n*-BuOH/benzene mixed solvent. The progress of the polymerization was monitored by tracing the change in the absorption spectrum of the reaction mixture at different time intervals (Figure S4, Supporting Information). **P1** and **P2** are relatively soluble in common organic solvents such as chloroform and THF.

Molecular weights of polymer **P1** were determined by gel permeation chromatography (GPC) using polystyrene standards as calibrants. The number-average molecular weight (M_n), weight-average molecular weight (M_w), and polydispersity index (M_w/M_n) of **P1** were 6298, 11 005, and 1.75, respectively.

Absorption Spectra. Figure 2 shows UV−vis−NIR absorption spectra of **P1** and **P2** in chloroform solution and in thin film. Figure S5 (Supporting Information) shows UV absorption spectra of **2** and **3** in chloroform solution. Compound **3** exhibits absorption maximum at 346 nm with a weak charge transfer band at ca. 500 nm. Compound **2** exhibits a red-shifted absorption maximum at 373 nm with a strong charge transfer band at ca. 547 nm due to increased conjugation. The small molecule **P2** in solution shows an intense and sharp absorption peak at 764 nm, and the absorption of the film is broadened and red-shifted remarkably, which is a typical phenomenon for squaraines resulted from strong charge transfer interactions and tendency to aggregation.[45] Relative to **3**, **P2** in solution exhibits a huge red shift (418 nm) of absorption maximum due to increased conjugation. Relative to **P2**, the polymer **P1** in solution exhibits red-shifted and broad absorption in visible and NIR region due to high degree of conjugation and planarity of the polymer, which is similar to other squaraine polymers.[37] The optical bandgap of **P1**, estimated from the absorption edge in films, is 0.97 eV, lower than that of its small molecule counterpart (1.27 eV, Table 1). The strong donor−acceptor interaction in these squaraines may be responsible for the observed long wavelength optical absorption. No fluorescence in **P1** and **P2** was observed probably due to strong intramolecular charge transfer between donor and acceptor units.

Electrochemistry. Cyclic voltammograms of the squaraine dyes **P1** and **P2** are illustrated in Figure 3, and the onset oxidation and reduction potentials of the materials are summarized in Table 2. Both compounds exhibit 1 oxidation peak and 3 reduction peaks. The potential of the Ag wire reference electrode was calibrated by internal standard ferrocene (E_{in} = 0.48 V versus Ag wire). The HOMO and LUMO energy levels were estimated from the onset oxidation and reduction potentials, assuming the absolute energy level of ferrocene/ferrocenium to be 4.8 eV below vacuum.[46] **P1** has an estimated HOMO of −5.02 eV and an estimated LUMO of −4.15 eV; **P2** has an estimated HOMO of −5.27 eV and an estimated LUMO of −3.22 eV. The higher HOMO and lower LUMO of **P1** indicates that the polymer is easier to oxidize and reduce than **P2** since the π-electrons are more delocalized along the polymer backbone.

Two-Photon Absorption at NIR Wavelengths. As we know, two-photon absorption (2PA) is a way of accessing a given excited state by using photons of nearly half the energy (or nearly

Scheme 1. Synthesis of Compounds P1 and P2

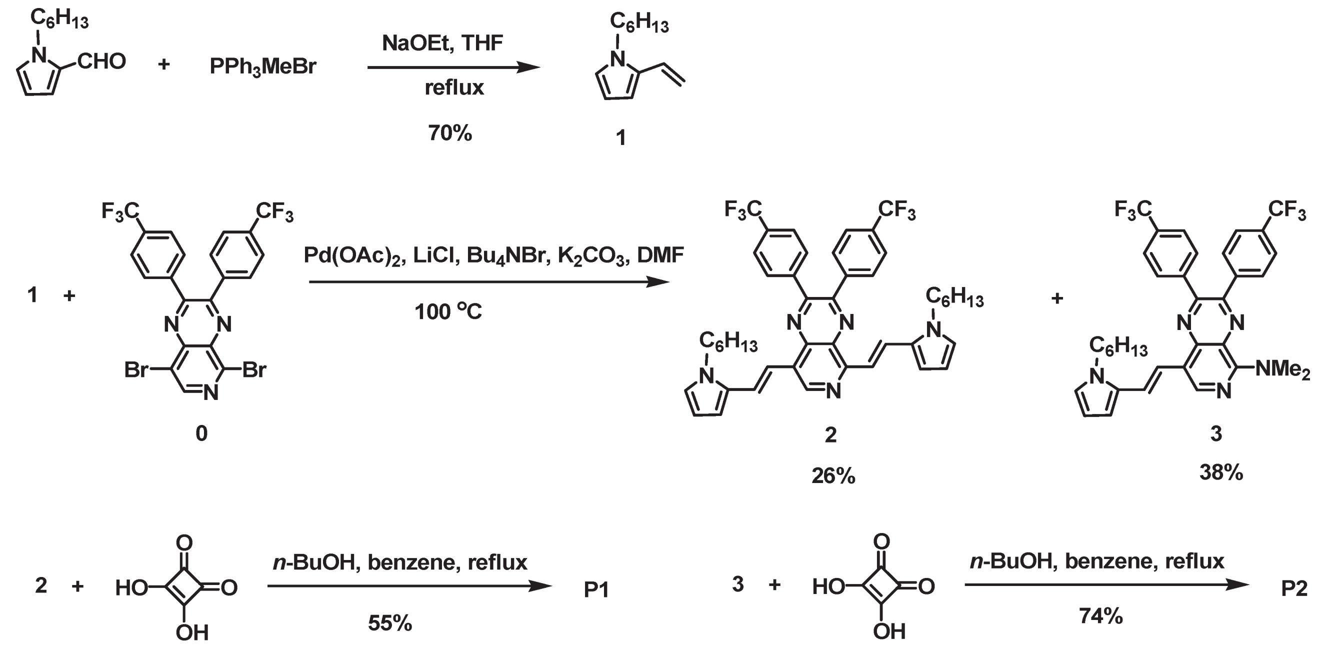

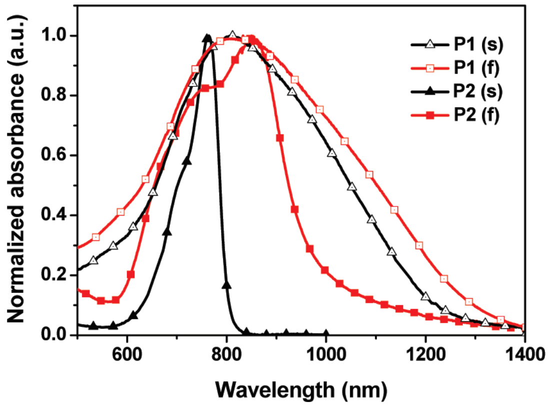

Figure 2. Absorption spectra of **P1** (10^{-6} M of repeat unit) and **P2** (10^{-6} M) in chloroform (s) and in thin film (f).

double the wavelength) of the corresponding one-photon transition. Since **P1** and **P2** in chloroform solution exhibit strong one-photon absorption at 764 and 808 nm, respectively, they may exhibit strong two-photon absorption at telecommunication wavelengths (1300−1550 nm). The 2PA cross sections (δ) of **P1** and **P2** were measured in the range of 1400−1640 nm in $CHCl_3$ by using the open-aperture Z-scan method. The typical Z-scan traces of **P1** and **P2** exhibit a clear dip (Figure 4). 2PA spectra of **P1** and **P2** in solution are shown in Figure 5. The 2PA cross sections and corresponding wavelengths are summarized in Table 3. Because of the extension of conjugation length, the 2PA cross sections per repeat unit of polymer **P1** are 1700−2300 GM, 3−5 times that for the small molecule **P2**.

■ CONCLUSION

In summary, we have synthesized two dicondensation products of pyridopyrazine-substituted pyrrole species with squaric acid, polymer **P1**, and small molecule **P2**. **P1** and **P2** exhibit strong NIR absorption and low bandgap. Compared to **P2**, **P1** exhibits higher HOMO and lower LUMO levels, red-shifted and broader absorption spectra, and lower bandgap due to higher degree of conjugation and delocalization of π-electrons. Polymer **P1** exhibits strong two-photon absorption at telecommunication wavelengths with 2PA cross sections per repeat unit as high as 2300 GM, 3−5 times that for the small molecule **P2** due to high degree of conjugation and delocalization of π-electrons in **P1**.

Table 1. Absorption Data of P1 and P2

	solution		film	
compd	$\lambda_{max}{}^{a}$ (nm)	ε^{b} (10^5 M^{-1} cm^{-1})	$\lambda_{max}{}^{a}$ (nm)	$E_g{}^{opt\ c}$ (eV)
P1	808	0.4	833	0.97
P2	764	2.14	850	1.27

[a] Absorption maxima. [b] Molar extinction coefficient (**P1** for repeat unit). [c] Optical bandgap was obtained from $E_g{}^{opt} = 1240/\lambda_{onset}$ (eV), wherein λ_{onset} is wavelength of its onset absorption edge in the longer wavelength direction.

■ EXPERIMENTAL SECTION

Materials. 1-Hexyl-1*H*-pyrrole-2-carbaldehyde[25] and 5,8-dibromo-2,3-bis(4-trifluoromethylphenyl)-pyrido[3,4-*b*]pyrazine[42] were synthesized according to the literature methods. Bio-Rad Bio-Beads S-X1 was purchased from Bio-Rad and used without further purification, which is neutral, porous styrene divinylbenzene beads for size exclusion chromatography of lipophilic polymers eluting with organic solvents. DMF was refluxed and distilled from calcium hydride. THF was distilled from sodium benzophenone under nitrogen before use. Unless stated otherwise, other reagents were purchased from commercial sources and used without further purification.

Characterization. The ^{1}H and ^{13}C NMR spectra were measured on a Bruker AVANCE 400 MHz spectrometer using tetramethylsilane

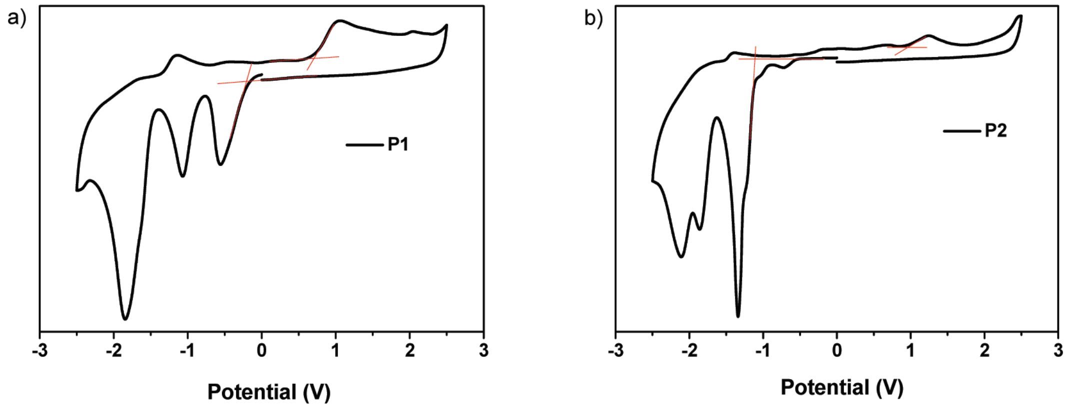

Figure 3. Cyclic voltammograms for **P1** and **P2** in CH_3CN/0.1 M $[^{n}Bu_4N]^+[PF_6]^-$ at 50 mV s^{-1}. The horizontal scale refers to an anodized Ag wire pseudoreference electrode.

Table 2. Redox Potentials and Energy Levels of P1 and P2[a]

	E_{ox}[b] (V)	E_{red}[b] (V)	E_{ox}[c] vs $FeCp_2^{+/0}$ (V)	E_{red}[c] vs $FeCp_2^{+/0}$ (V)	HOMO[d] (eV)	LUMO[d] (eV)
P1	+0.70	−0.17	+0.22	−0.65	−5.02	−4.15
P2	+0.95	−1.10	+0.47	−1.58	−5.27	−3.22

[a] Thin films on glassy-carbon electrode in CH_3CN/0.1 M $[^{n}Bu_4N]^+[PF_6]^-$ at 50 mV s^{-1}. [b] E_{ox} is the onset potentials versus anodized Ag wire pseudoreference electrode corresponding to oxidations, while E_{red} is the onset potentials versus anodized Ag wire pseudoreference electrode corresponding to reductions. [c] E_{ox} vs $FeCp_2^{+/0} = E_{ox} - E_{in}$, E_{red} vs $FeCp_2^{+/0} = E_{red} - E_{in}$. [d] HOMO $= -e(E_{ox}$ vs $FeCp_2^{+/0} + 4.8)$ (eV), LUMO $= -e(E_{red}$ vs $FeCp_2^{+/0} + 4.8)$ (eV).

(TMS; $\delta = 0$ ppm) as an internal standard. The selective 1D NOE NMR and HSQC 2D NMR spectra were measured on a Bruker AVANCE 600 MHz spectrometer. Mass spectra were measured on a GCT-MS micromass spectrometer using the electron impact (EI) mode or on a Bruker Daltonics BIFLEX III MALDI-TOF Analyzer using MALDI mode. Elemental analyses were carried out using a FLASH EA1112 elemental analyzer. Solution (chloroform) and thin-film (on quartz substrate) UV−vis−NIR absorption spectra were recorded on a JASCO V-570 spectrophotometer. Electrochemical measurements were carried out under nitrogen on a deoxygenated solution of tetra-*n*-butylammonium hexafluorophosphate (0.1 M) in acetonitrile using a computer-controlled Zahner IM6e electrochemical workstation, a glassy-carbon working electrode coated with sample films, a platinum-wire auxiliary electrode, and an Ag wire anodized with AgCl as a pseudoreference electrode. Potentials were referenced to the ferrocenium/ferrocene ($FeCp_2^{+/0}$) couple by using ferrocene as an internal standard. Thermogravimetric analysis (TGA) measurements were performed on Shimadzu thermogravimetric analyzer (model DTG-60) under a nitrogen flow at a heating rate of 10 °C min^{-1}. The gel permeation chromatography (GPC) measurements were performed on a Waters 515 chromatograph connected to a Waters 2414 refractive index detector, using THF as eluent and polystyrene standards as calibrants, three Waters Styragel columns (HT2, -3, -4) connected in series were used.

2PA Measurement. The 2PA cross sections δ of **P1** and **P2** were measured at 1520, 1560, and 1640 nm in $CHCl_3$ by using the open-aperture Z-scan method,[47,48] with ~120 fs pulses from an optical parametric amplify (OPA) operating at a 1 kHz repetition rate generated from a mode-locked Ti:sapphire femtosecond laser (Tsunami, Spectra-Physics). The laser beam was divided into two parts. One was used as the intensity reference and monitored by EPM 2000 power meter (Coherent Inc.). The other was used for transmittance measurement; the laser beam was focused by passing through lens (f = 15 cm) and passed through a quartz cell with a sample thickness of 1 mm. The position of the sample cell could be varied along the laser-beam direction (z-axis), so the local power density within the sample cell could be changed under a constant laser power level. The transmitted laser beam from the sample cell was then detected by the same power meter as used for reference monitoring. The on-axis peak intensity of the incident pulses at the focal point, I_0, ranged from 41 to 46 GW cm^{-2}. Assuming a Gaussian beam profile, the nonlinear absorption coefficient β can be obtained by curve fitting to the observed open-aperture traces with eq 1.

$$T(z) = 1 - \frac{\beta I_0(1 - e^{-\alpha_0 l})}{2\alpha_0(1 + (z/z_0)^2)} \qquad (1)$$

where α_0 is the linear absorption coefficient, l the sample length, and z_0 the diffraction length of the incident beam. We obtained the nonlinear absorption coefficient β at the corresponding wavelength, where linear absorption is negligible, to satisfy the condition of $\alpha_0 l \ll 1$. When $\alpha_0 l \ll 1$, eq 1 can be simplified as eq 2.

$$T(z) = 1 - \frac{\beta I_0 l}{2(1 + (z/z_0)^2)} \qquad (2)$$

The 2PA cross section δ of **P1** and **P2** (in units of 1 GM = 1×10^{-50} cm^4 s^{-1}) can be determined by eq 3.

$$\beta = \frac{\delta N_A d \times 10^{-3}}{h\nu} \qquad (3)$$

where N_A is the Avogadro constant, d is the concentration of the repeated unit of **P1** and **P2** in $CHCl_3$ (the corresponding concentrations for **P1** and **P2** are 2.8×10^{-4} and 1.6×10^{-4} M, respectively), h is the Planck constant, and ν is the frequency of the incident laser beam.

1-Hexyl-2-vinyl-1*H*-pyrrole (1). To a 100 mL three-neck round-bottom flask, dry THF (20 mL) was charged under N_2 flow. NaOEt (1.836 g, 27 mmol) and PPh_3MeBr (8.9 g, 25 mmol) were added. The mixture was stirred at room temperature for 3 h. Then a solution of 1-hexyl-1*H*-pyrrole-2-carbaldehyde (4.475 g, 25 mmol) in 10 mL of THF was added dropwise. After the reaction mixture was stirred under

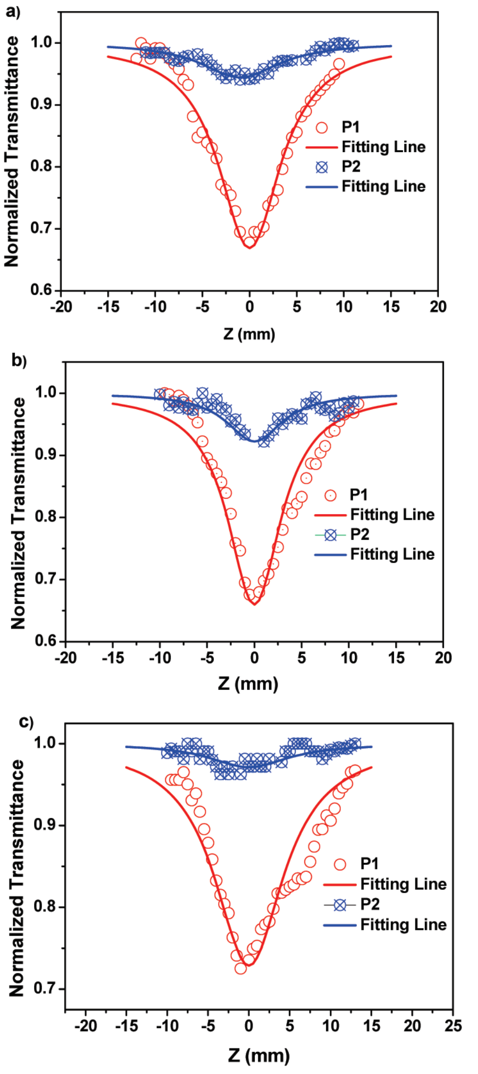

Figure 4. Z-scan traces (circle) of **P1** (2.8×10^{-4} M per repeat unit) and **P2** (1.6×10^{-4} M) in $CHCl_3$ in a 1 mm cell at (a) 1640 nm (I_0 = 41.0 GW cm^{-2}), (b) 1560 nm (I_0 = 44.0 GW cm^{-2}), and (c) 1520 nm (I_0 = 46.0 GW cm^{-2}) with a theoretical fit assuming a 2PA process (solid line).

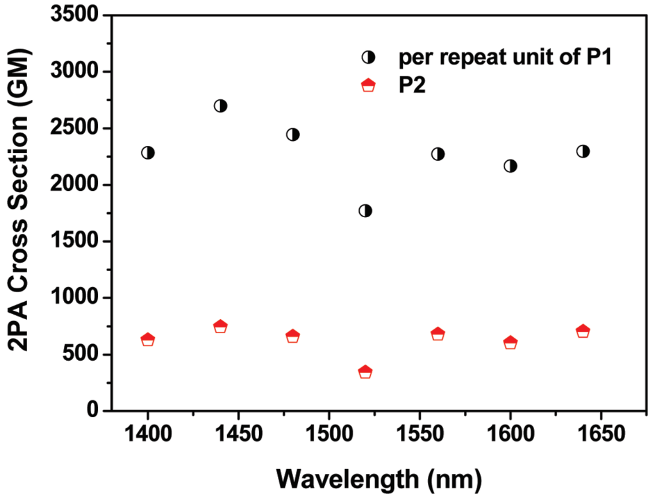

Figure 5. 2PA spectra for **P1** and **P2** in the range of 1400−1640 nm.

Table 3. 2PA Cross Sections at Telecommunication Wavelengths for P1 (per Repeat Unit) and P2

	δ (GM) at 1520 nm	δ (GM) at 1560 nm	δ (GM) at 1640 nm
P1	1770	2271	2300
P2	343	679	704

reflux for 15 h, the THF was removed under vacuum and the residue was suspended in CH_2Cl_2 and filtered. The filtrate was extracted with 50 mL of $NaHSO_3$ solution (15 g of $NaHSO_3$ in water), 50 mL of Na_2CO_3 solution (10 g of Na_2CO_3 in water), and 50 mL of H_2O. After that the organic phase was dried over Na_2SO_4, and the solvent was removed under vacuum. Purification by column chromatography (silica gel, hexanes) afforded colorless oil (3.1 g, 70%). ^{1}H NMR (400 MHz, $CDCl_3$): δ 6.63 (s, 1H), 6.58 (t, J = 8.8 Hz, 1H), 6.40 (t, J = 1.7 Hz, 1H), 6.12 (t, J = 2.9 Hz, 1H), 5.53 (d, J = 17.3 Hz, 1H), 5.06 (d, J = 11.2 Hz, 1H), 3.89 (t, J = 7.3 Hz, 2H), 1.71 (m, 2H), 1.31 (m, 6H), 0.90 (t, J = 6.3 Hz, 3H). HRMS (EI): *m*/*z* cacld for $C_{12}H_{19}N$: 177.1517, found: 177.1514. Anal. Calcd for $C_{12}H_{19}N$: C, 81.30; H, 10.80; N, 7.90. Found: C, 81.02; H, 10.77; N, 7.77%.

5,8-Bis((*E*)-2-(1-hexyl-1*H*-pyrrol-2-yl)vinyl)-2,3-bis(4-(trifluoromethyl)phenyl)pyrido[3,4-*b*]pyrazine (2). To a 50 mL three-neck flask, 5,8-dibromo-2,3-bis(4-trifluoromethylphenyl)pyrido[3,4-*b*]-pyrazine (287.45 mg, 0.5 mmol), K_2CO_3 (1.034 g, 7.5 mmol), Bu_4NBr (240.9 mg, 0.75 mmol), LiCl (31.5 mg, 0.75 mmol), and $Pd(OAc)_2$ (16.8 mg, 0.075 mmol) were added and deoxygenated with nitrogen for 30 min. Compound **1** (265.7 mg, 1.5 mmol) in anhydrous DMF (15 mL) was added directly, and the red mixture was stirred at 100 °C for 24 h. The mixture was cooled to room temperature, washed with water, extracted with dichloromethane, and dried over $MgSO_4$. Purification by column chromatography (silica gel, CH_2Cl_2:hexanes = 1:1) afforded a purple solid (100 mg, 26%). ^{1}H NMR (400 MHz, $CDCl_3$): δ 8.95 (s, 1H), 8.26 (d, J = 15.5 Hz, 1H), 8.12 (d, J = 15.7 Hz, 1H), 7.82 (d, J = 16.3 Hz, 1H), 7.78 (d, J = 7.7 Hz,, 4H), 7.72 (d, J = 7.7 Hz,, 4H), 7.63 (d, J = 16.3 Hz, 1H), 6.84 (s, 1H), 6.81 (s, 1H), 6.74 (s, 1H), 6.70 (s, 1H), 6.24 (s, 1H), 6.22 (s, 1H), 4.11 (t, J = 7.3 Hz, 2H), 3.99 (t, J = 7.3 Hz, 2H), 1.83 (m, 2H), 1.73 (m, 2H), 1.31 (m, 6H), 1.24 (m, 6H), 0.88 (t, J = 6.3 Hz, 3H), 0.85 (t, J = 5.9 Hz, 3H). HRMS (EI): *m*/*z* cacld for $C_{45}H_{45}F_6N_5$: 769.3579, found: 769.3588. Anal. Calcd for $C_{45}H_{45}F_6N_5$: C, 70.20; H, 5.89; N, 9.10. Found: C, 69.83; H, 5.76; N, 8.97%. This compound was further confirmed by HSQC 2D NMR (Figure S6, Supporting Information).

(*E*)-8-(2-(1-Hexyl-1*H*-pyrrol-2-yl)vinyl)-5-dimethylamino)-2,3-bis(4-(trifluoromethyl)phenyl)pyrido[3,4-*b*]pyrazine (3). The same procedure as **2** to afford a red solid (120 mg, 38%). ^{1}H NMR (400 MHz, $CDCl_3$): δ 8.51 (s, 1H), 7.78 (d, J = 7.9 Hz, 2H), 7.63 (m, 6H), 7.47 (dd, J = 21.2 Hz, 4.8 Hz, 2H), 6.68 (s, 1H), 6.57 (s, 1H), 6.18 (s, 1H), 3.96 (t, J = 7.1 Hz, 2H), 3.59 (s, 6H), 1.71 (m, 2H), 1.23 (m, 6H), 0.83 (t, J = 6.4 Hz, 3H). The structure was further certified by selective 1D NOE NMR (Figures S1−3, Supporting Information) and HSQC 2D NMR (Figure S7, Supporting Information). HRMS (EI): *m*/*z* cacld for $C_{35}H_{33}F_6N_5$: 637.2640, found: 637.2648. Anal. Calcd for $C_{35}H_{33}F_6N_5$: C, 65.92; H, 5.22; N, 10.98. Found: C, 65.53; H, 5.14; N, 10.88%.

Polymer P1. To a 50 mL three-neck flask, squaric acid (17.4 mg, 0.15 mmol) and compound **2** (115 mg, 0.15 mmol) were added. A mixture of *n*-butanol (4 mL) and benzene (8 mL) was added, and the reaction mixture was refluxed under a nitrogen atmosphere for 11 h. After the reaction mixture was cooled to room temperature, the polymer was precipitated by addition of 100 mL of methanol. Finally, the polymer was purified by size exclusion column chromatography over Bio-Rad

Bio-Beads S-X1 eluting with chloroform. The polymer was recovered as a black solid from the chloroform fraction by rotary evaporation (70 mg, 55%). ^{1}H NMR (400 MHz, CD_2Cl_2): δ 8.20 (br, 1H), 7.65 (br, 12H), 7.10 (br, 4H), 4.13 (br, 2H), 3.78 (br, 2H), 2.33 (br, 2H), 2.02 (br, 2H), 1.55−1.26 (br, 12H), 0.88 (br, 6H) (Figure S8, Supporting Information). GPC: M_n, 6298; M_w, 11 005; M_w/M_n, 1.75. Anal. Calcd for $(C_{49}H_{43}F_6N_5O_2)_n$: C, 69.41; H, 5.11; N, 8.26. Found: C, 64.14; H, 6.06; N, 7.31%.

Compound P2. To a 50 mL three-neck flask, squaric acid (8.12 mg, 0.07 mmol) and compound **3** (127.45 mg, 0.2 mmol) were added. A mixture of *n*-butanol (2 mL) and benzene (4 mL) was added, and the reaction mixture was refluxed under a nitrogen atmosphere for 11 h. The mixture was cooled to room temperature, washed with water, and extracted with dichloromethane, and the organic phase was dried over $MgSO_4$. Purification by column chromatography (silica gel, CH_2Cl_2) afforded a green solid (70 mg, 74%). ^{1}H NMR (400 MHz, $CDCl_3$): δ 8.55 (br, 2H), 7.87 (br, 4H), 7.72−7.64 (br, 12H), 7.52 (br, 4H), 7.01 (br, 4H), 4.85 (br, 4H), 3.67 (br, 12H), 1.85 (m, 4H), 1.40 (m, 12H), 0.86 (m, 6H) (Figure S9, Supporting Information). MS (MALDI): *m/z* 1352 (M^+). Anal. Calcd for $C_{74}H_{64}F_{12}N_{10}O_2$: C, 65.67; H, 4.77; N, 10.35. Found: C, 65.33; H, 4.74; N, 10.18%.

■ ASSOCIATED CONTENT

Ⓢ **Supporting Information.** Effect of compound **1**:compound **0** mole ratio on products; ^{1}H NMR, selective 1D NOE and HSQC NMR spectra of **3**; HSQC spectrum of **2**; ^{1}H NMR spectra of **P1** and **P2**; absorption spectra of polysquaraine varying with reaction time; absorption spectra of compounds **2** and **3** in chloroform solution. This material is available free of charge via the Internet at http://pubs.acs.org.

■ AUTHOR INFORMATION

Corresponding Author

*E-mail: xwzhan@iccas.ac.cn (X.Z.), xmduan@mail.ipc.ac.cn (X.-M.D.).

■ ACKNOWLEDGMENT

This work was supported by NSFC (Grants 21025418 and 21021091), 973 Project (Grant 2011CB808401), and the Chinese Academy of Sciences.

■ REFERENCES

(1) Büschel, M.; Ajayaghosh, A.; Arunkumar, E.; Daub, J. *Org. Lett.* **2003**, *5*, 2975.

(2) Jyothish, K.; Arun, K. T.; Ramaiah, D. *Org. Lett.* **2004**, *6*, 3965.

(3) Sreejith, S.; Carol, P.; Chithra, P.; Ajayaghosh, A. *J. Mater. Chem.* **2008**, *18*, 264.

(4) Ajayaghosh, A. *Acc. Chem. Res.* **2005**, *38*, 449.

(5) Beverina, L.; Salice, P. *Eur. J. Org. Chem.* **2010**, *2010*, 1207.

(6) Treibs, A.; Jacob, K. *Angew. Chem., Int. Ed. Engl.* **1965**, *4*, 694.

(7) Law, K. Y. *Chem. Rev.* **1993**, *93*, 449.

(8) Emmelius, M.; Pawlowski, G.; Vollmann, H. *Angew. Chem., Int. Ed. Engl.* **1989**, *28*, 1445.

(9) Smits, E. C. P.; Setayesh, S.; Anthopoulos, T. D.; Buechel, M.; Nijssen, W.; Coehoorn, R.; Blom, P. W. M.; de Boer, B.; de Leeuw, D. M. *Adv. Mater.* **2007**, *19*, 734.

(10) Chen, C. T.; Marder, S. R.; Cheng, L. T. *J. Am. Chem. Soc.* **1994**, *116*, 3117.

(11) Silvestri, F.; Irwin, M. D.; Beverina, L.; Facchetti, A.; Pagani, G. A.; Marks, T. J. *J. Am. Chem. Soc.* **2008**, *130*, 17640.

(12) Yum, J. H.; Walter, P.; Huber, S.; Rentsch, D.; Geiger, T.; Nuesch, F.; De Angelis, F.; Gratzel, M.; Nazeeruddin, M. K. *J. Am. Chem. Soc.* **2007**, *129*, 10320.

(13) Liu, L. H.; Nakatani, K.; Pansu, R.; Vachon, J. J.; Tauc, P.; Ishow, E. *Adv. Mater.* **2007**, *19*, 433.

(14) Arunkumar, E.; Forbes, C. C.; Noll, B. C.; Smith, B. D. *J. Am. Chem. Soc.* **2005**, *127*, 3288.

(15) Johnson, J. R.; Fu, N.; Arunkumar, E.; Leevy, W. M.; Gammon, S. T.; Piwnica-Worms, D.; Smith, B. D. *Angew. Chem., Int. Ed.* **2007**, *46*, 5528.

(16) Arunkumar, E.; Ajayaghosh, A.; Daub, J. *J. Am. Chem. Soc.* **2005**, *127*, 3156.

(17) Arunkumar, E.; Chithra, P.; Ajayaghosh, A. *J. Am. Chem. Soc.* **2004**, *126*, 6590.

(18) Beverina, L.; Crippa, M.; Landenna, M.; Ruffo, R.; Salice, P.; Silvestri, F.; Versari, S.; Villa, A.; Ciaffoni, L.; Collini, E.; Ferrante, C.; Bradamante, S.; Mari, C. M.; Bozio, R.; Pagani, G. A. *J. Am. Chem. Soc.* **2008**, *130*, 1894.

(19) He, G. S.; Tan, L. S.; Zheng, Q.; Prasad, P. N. *Chem. Rev.* **2008**, *108*, 1245.

(20) Rumi, M.; Barlow, S.; Wang, J.; Perry, J. W.; Marder, S. R. *Adv. Polym. Sci.* **2008**, *213*, 1.

(21) Terenziani, F.; Katan, C.; Badaeva, E.; Tretiak, S.; Blanchard-Desce, M. *Adv. Mater.* **2008**, *20*, 4641.

(22) Kim, H. M.; Cho, B. R. *Chem. Commun.* **2009**, 153.

(23) Pawlicki, M.; Collins, H. A.; Denning, R. G.; Anderson, H. L. *Angew. Chem., Int. Ed.* **2009**, *48*, 3244.

(24) Scherer, D.; Dorfler, R.; Feldner, A.; Vogtmann, T.; Schwoerer, M.; Lawrentz, U.; Grahn, W.; Lambert, C. *Chem. Phys.* **2002**, *279*, 179.

(25) Chung, S. J.; Zheng, S. J.; Odani, T.; Beverina, L.; Fu, J.; Padilha, L. A.; Biesso, A.; Hales, J. M.; Zhan, X. W.; Schmidt, K.; Ye, A. J.; Zojer, E.; Barlow, S.; Hagan, D. J.; Van Stryland, E. W.; Yi, Y. P.; Shuai, Z. G.; Pagani, G. A.; Bredas, J. L.; Perry, J. W.; Marder, S. R. *J. Am. Chem. Soc.* **2006**, *128*, 14444.

(26) Odom, S. A.; Webster, S.; Padilha, L. A.; Peceli, D.; Hu, H.; Nootz, G.; Chung, S.-J.; Ohira, S.; Matichak, J. D.; Przhonska, O. V.; Kachkovski, A. D.; Barlow, S.; Brédas, J.-L.; Anderson, H. L.; Hagan, D. J.; Van Stryland, E. W.; Marder, S. R. *J. Am. Chem. Soc.* **2009**, *131*, 7510.

(27) Webster, S.; Odom, S. A.; Padilha, L. A.; Przhonska, O. V.; Peceli, D.; Hu, H. H.; Nootz, G.; Kachkovski, A. D.; Matichak, J.; Barlow, S.; Anderson, H. L.; Marder, S. R.; Hagan, D. J.; Van Stryland, E. W. *J. Phys. Chem. B* **2009**, *113*, 14854.

(28) Beverina, L.; Crippa, M.; Salice, P.; Ruffo, R.; Ferrante, C.; Fortunati, I.; Signorini, R.; Mari, C. M.; Bozio, R.; Facchetti, A.; Pagani, G. A. *Chem. Mater.* **2008**, *20*, 3242.

(29) Ohira, S.; Rudra, I.; Schmidt, K.; Barlow, S.; Chung, S.-J.; Zhang, Q.; Matichak, J.; Marder, S. R.; Brédas, J.-L. *Chem.—Eur. J.* **2008**, *14*, 11082.

(30) Ajayaghosh, A. *Chem. Soc. Rev.* **2003**, *32*, 181.

(31) Brocks, G.; Tol, A. *J. Phys. Chem.* **1996**, *100*, 1838.

(32) Chen, Y.; Hall, H. *Polym. Bull.* **1986**, *16*, 419.

(33) Havinga, E.; Hoeve, W.; Wynberg, H. *Polym. Bull.* **1992**, *29*, 119.

(34) Chenthamarakshan, C. R.; Eldo, J.; Ajayaghosh, A. *Macromolecules* **1999**, *32*, 251.

(35) Chenthamarakshan, C. R.; Ajayaghosh, A. *Chem. Mater.* **1998**, *10*, 1657.

(36) Ajayaghosh, A.; Chenthamarakshan, C. R.; Das, S.; George, M. V. *Chem. Mater.* **1997**, *9*, 644.

(37) Ajayaghosh, A.; Eldo, J. *Org. Lett.* **2001**, *3*, 2595.

(38) Chenthamarakshan, C. R.; Ajayaghosh, A. *Tetrahedron Lett.* **1998**, *39*, 1795.

(39) Chenthamarakshan, C. R.; Eldo, J.; Ajayaghosh, A. *Macromolecules* **1999**, *32*, 5846.

(40) Kaafarani, B. R.; Kondo, T.; Yu, J.; Zhang, Q.; Dattilo, D. C.; Risko, C.; Jones, S. C.; Barlow, S.; Domercq, B.; Amy, F.; Kahn, A.; Brédas, J.-L.; Kippelen, B.; Marder, S. R. *J. Am. Chem. Soc.* **2005**, *127* 16358.

(41) Naraso, Nishida, J.; Kumaki, D.; Tokito, S.; Yamashita, Y. *J. Am. Chem. Soc.* **2006**, *128*, 9598.

(42) Wang, H.; Wen, Y.; Yang, X.; Wang, Y.; Zhou, W.; Zhang, S.; Zhan, X.; Liu, Y.; Shuai, Z.; Zhu, D. *ACS Appl. Mater. Interfaces* **2009**, *1*, 1122.

(43) Huang, X.; Shi, Q.; Chen, W.-Q.; Zhu, C.; Zhou, W.; Zhao, Z.; Duan, X.-M.; Zhan, X. *Macromolecules* **2010**, *43*, 9620.

(44) Delia, T. J.; Meltsner, B. R.; Schomaker, J. M. *J. Heterocycl. Chem.* **1999**, *36*, 1259.

(45) Toro, C.; De Boni, L.; Yao, S.; Ritchie, J. P.; Masunov, A. m. E.; Belfield, K. D.; Hernandez, F. E. *J. Chem. Phys.* **2009**, *130*, 214504.

(46) Pommerehne, J.; Vestweber, H.; Guss, W.; Mahrt, R. F.; Bassler, H.; Porsch, M.; Daub, J. *Adv. Mater.* **1995**, *7*, 551.

(47) Wei, T. H.; Hagan, D. J.; Sense, M. J.; Van Stryland, E. W.; Perry, J. W.; Coulter, D. R. *Appl. Phys. B: Lasers Opt.* **1992**, *54*, 46.

(48) Sheik-Bahae, M.; Said, A. A.; Wei, T.-H.; Hagan, D. J.; Van Stryland, E. W. *IEEE J. Quantum Electron.* **1990**, *26*, 760.